2025 AWES Undergraduate Wind Engineering Prize

Cover Sheet

Title of Thesis / Project: Wind Loads on Tilted Solar Panels Mounted on Low-Pitch Monoslope Roofs

Name(s) and Email of Student Author(s): Ronan Dobson, ronan.dobson@my.jcu.edu.au

Name(s) and Email of Supervisor(s): Dr. Juan Zaracho, juanignacio.zaracho@jcu.edu.au

Mr. Simon Ingham, simon.ingham@jcu.edu.au

Declaration

This submission is a summary of the Final Year Thesis/Project carried out by the Author(s) at *James Cook University* in the academic year of 2025. This submission is prepared by the Author(s) alone.

Ronan Dobson
Student name(s)

R.D
Signature(s)

Relevance to Wind Engineering

Describe the relevance of your thesis to the field of Wind Engineering (200-word limit).

Rooftop solar installations are rapidly increasing across Australia, yet their wind loading behaviour remains partially understood, particularly when panels are mounted at a tilt angle on low-pitch residential roofs. Recent cyclones, including Debbie (2017) and Ilsa (2023), have demonstrated that solar arrays can exacerbate roof failure by introducing complex aerodynamic effects not represented in current design standards. AS/NZS 1170.2 provides contains no provisions for tilted solar panels, despite their widespread use. As a result, structural engineers must rely on assumptions that may significantly under-estimate wind actions on roofs fitted with solar arrays.

This paper directly addresses this gap through wind tunnel testing of tilted panel arrays mounted on a 5° monoslope roof, using a 1:20 scale model designed to represent typical Australian housing. Measurements focus on the critical corner region and examine two typical array configurations: a fully covered roof and a high-eave-single array. The results reveal aerodynamic mechanisms that amplify uplift and demonstrate where AS/NZS 1170.2 does not capture the observed wind loads. The findings provide new experimental evidence that can inform future revisions of Australian wind loading provisions.

Wind Loads on Tilted Solar Panels Mounted on Low-Pitch Monoslope Roofs

Ronan Dobson

INTRODUCTION

Rooftop solar adoption in Australia has expanded rapidly over the past decade, driven by increasing emphasis on renewable energy supply (ARENA, 2023). However, this growth has outpaced the development of wind design guidance. Solar arrays mounted on low-rise housing have been repeatedly damaged or detached during severe wind events, with Cyclones Debbie (2017) and Ilsa (2023) revealing cases where solar systems contributed to progressive roof failure as seen in Figure 1 (a). These failures underscore the importance of understanding how tilted panels modify local aerodynamic loads.

AS/NZS 1170.2 provides wind loading data for panels installed parallel to the roofs surface but includes no design provisions for solar panels inclined to the roof like those shown in Figure 1 (b). Prior research has focused on flat roofs or idealised panel arrangements, leaving a gap in experimental data for low-pitch residential roofs.

(a) **(b)**

Figure 1. (a) Cyclone Debbie Rooftop Failure (Boughton, 2017) and (b) Tilted Solar Arrays in the Gold Coast, Australia (Cyclone Testing Station, 2025)

This paper summarises the Final Year Thesis work on wind loads on tilted solar panel arrays mounted on a 5° monoslope roof. Analysis within the thesis compares 6 typical PV-array layouts.

The objectives were to characterise flow behaviour and resulting pressure distributions for panel tilt angles $\alpha = 10°$, 20°, and 30°, to compare aerodynamic mechanisms between the two configurations, and to evaluate the suitability of current AS/NZS 1170.2 provisions for these systems.

METHODOLOGY

Wind tunnel testing was conducted at the Cyclone Testing Station, James Cook University, Townsville, Australia. A suburban exposure profile of Terrain Category 2.5 was simulated using floor roughness blocks to match the target velocity and turbulence intensity profiles.

A 1:20 scaled model of a low rise, 5° monoslope roof building was utilised. Six solar panel array configurations were tested.

The roof surface incorporated 99 pressure taps arranged across half the roof. Pressure taps were fitted to both the top and bottom surface of the instrumented model panels. This allowed measuring time-varying top ($p_t(t)$) and bottom ($p_b(t)$) pressures to provide a net pressure, $p_n(t) = (p_t(\mathrm{t}) - p_b(t))$. Details of the model are given in Figure 2:

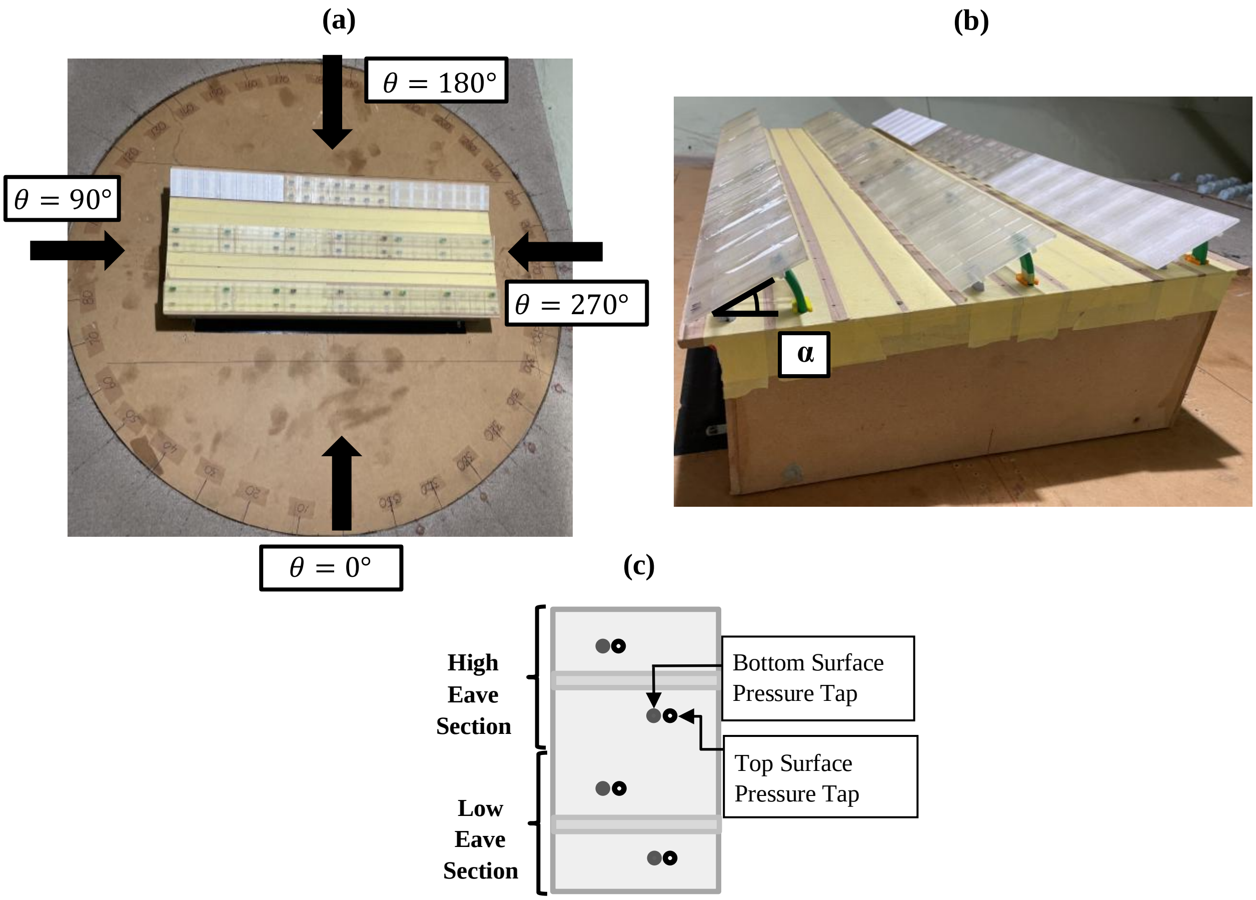

Figure 2 (a) Model Plan View Indicating Wind Direction (θ), (b) Model Elevation View Indicating Tilt Angle (α), (c) Pressure Tap Layout on Panel Model

The distribution of pressure taps allowed the analysis of intra panel loading between high and low eave panel sections.

Pressure time histories ($p(t)$) were recorded at 500 Hz using a Pitot tube located at 500mm (10m in full-scale), for wind direction θ ranging from 0° to 360°, in 10°. Pressures were converted to dimensionless coefficients as shown in Equation 1. Mid-roof height pressure ($C_{p,h}$) shape factors $\left(C_{shp}\right)$ were computed based on the Gust Factor (G_u) as per Equation 2:

$$C_{p,h}(t) = \frac{p(t)}{\frac{1}{2}\rho \bar{V}_{p,h}^2} = \frac{C_{500}}{\left(\frac{V_{p,h}}{V_{500}}\right)^2} \qquad \textbf{Eq. 1}$$

$$C_{shp}(t) = \frac{C_{p,h}}{G_u^2} \qquad \textbf{Eq. 2}$$

The study comprised several configurations from which two of them are analysed in this paper. These configurations (i.e., Configurations 6 and 7) are shown in Figure 3. Configuration 6 represents a full roof coverage, including dummy panels (panels which record no data) to replicate multi-row arrays. Configurations 7 refers to a single array located on the high-eave region, leaving the low eave unobstructed. Panel tilt angle α = 10°, 20°, and 30° were tested.

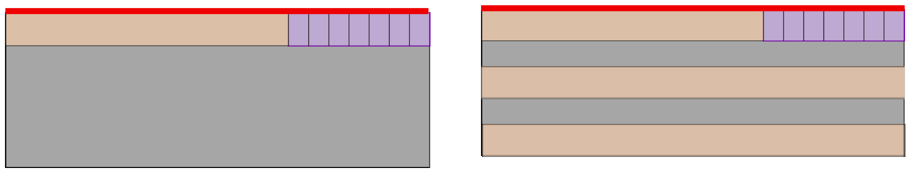

(a) Configuration 7– Corner Located High Eave Dummy

(b) Configuration 6– Corner Located Dummy Panel Covered

	Instrumented Panel
	Dummy Panel
	Roof High Eave

Figure 3. Plan View of (a) Configurations 6 and (b) Configuration 7

RESULTS AND DISCUSSION

This section presents the influence of both panel tilt and array density on the uplift behaviour of tilted solar arrays. The measured loads are subsequently evaluated against AS/NZS 1170.2.

Effect of Panel Tilt

Figure 4 shows the variation of mean. Pressure coefficients against wind direction for different tilt angles at the low and high eave sections of the panel.

(a) **(b)**

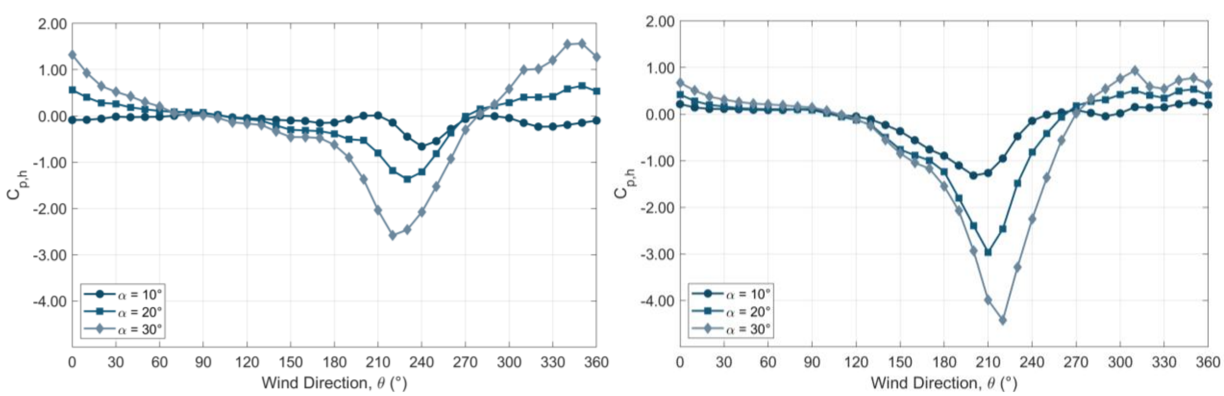

Figure 4. Pressure coefficients vs Wind direction on (a) Panel Low eave and (b) Panel High Eave , for α = 10°, 20° and 30°

For normal wind directions (i.e. θ ≈ 180° –230°) α = 20° and 30° produce a particular increase in suction. This occurs because the increase in tilt angle strengthens flow separation. At α = 30°, uplift is greatest, with suction magnitudes increasing by up to 370% relative to α = 10°.

Conversely, crosswind directions show small variation of pressure with tilt angle changes, as the flow remains broadly aligned with the panel surface and behaves in a more streamlined manner. For these orientations, flow separation is limited, and the normal-force contribution is small. Tilt-driven uplift force amplification is therefore highly dependent on wind direction θ, with the higher increments occurring under normal wind incidence.

Effect of Array Coverage

The influence of array coverage on panel loading is demonstrated in Figure 5 for (a) α = 10° and (b) α = 30°, which compare mean net pressure coefficients for Configuration 6 (with upstream dummy panels) and Configuration 7 (no upstream panels). At low tilt angle, the presence of upstream panels produces a flow amplification effect.

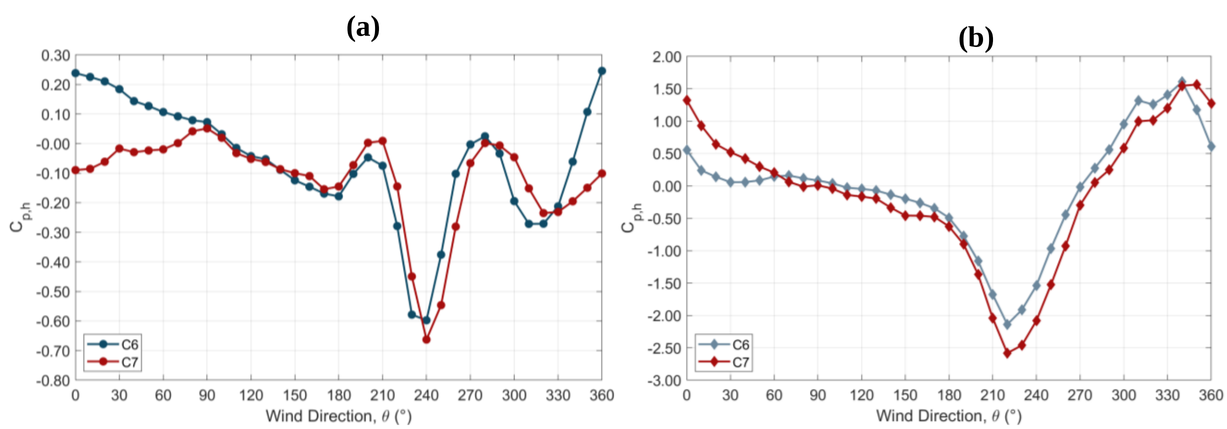

Figure 5. Pressure coefficient $C_{p,h}$ vs Wind direction (θ) for (a) α = 10° and (b) α = 30°

At α = 10°, the presence of upstream panels produces coverage-induced amplification, seen as elevated net positive pressure coefficients in Configuration 6 whilst $\theta \approx 0°$. The upstream rows accelerate the flow within the roof–panel cavity, increasing loading on the downstream panel relative to Configuration 7.

At higher tilt angles (i.e α = 20° and 30°), flow shielding dominates. As observed in Figure 5 (b), Configuration 7 exhibits elevated pressures than Configuration 6 whilst $\theta \approx 0°$.

Comparison With AS/NZS 1170.2

AS/NZS 1170.2 Appendix B.6 provides shape coefficients for solar panels parallel to the roof. Table 1 shows these coefficients together with peak experimental C_{shp} values from the edge panel.

The differences are dependent on wind direction θ and tilt angle α. For θ = 0° and 270°, the Standard provides lower uplift shape coefficients, particularly at lower tilt angles (i.e. α = 10°). At θ = 180°, however, uplift increases rapidly with tilt angle, producing larger loads at α = 20° and 30° due to stronger flow separation. Positive pressure also varies: at α = 10°, the Standard typically presents higher pressures due to stagnation, whereas at higher tilt angle the experimental values exceed the Standard, most notably at θ = 0° for α = 30°.

Table 1. Shape coefficients C_{shp} extracted from AS/NZ1170.2 and Peak Experimental C_{shp} for several tilt angles

θ (°)	AS/NZS1170.2	α = 10°	α = 20°	α = 30°
180 (Upwind End)	-1.1, +0.8	-1.24, +0.38	-1.72, +0.28	-2.22, +0.31
0 (Downwind End)	-1.1, +0.5	-0.39, +0.46	-0.22, +0.83	-0.25, +1.24
270 (Upwind End)	-1.7, +0.4	-0.68, +0.44	-0.97, +0.47	-1.50, +0.74

Overall, the comparison highlights that tilt and array orientation introduce aerodynamic behaviors not represented in AS/NZS 1170.2, resulting in direction- and tilt-specific differences between experimental and design coefficients.

CONCLUSIONS

- Tilted solar panels significantly alter roof aerodynamics, producing higher wind load patterns compared to low-pitch roofs.
- Increasing tilt angle α from 10° to 30° results in increments in uplift, with the greatest increase occurring when the approaching wind direction θ is near-normal to the panel surface.
- Array density influences uplift directionally—continuous coverage (Configuration 6) enhances under-array flow and uplift at low tilt, whereas sparse layouts expose the panel high eave and generate sharper, more localised suction peaks at higher tilt angles.
- Wind direction is a major driver of aerodynamic loading, with the most critical uplift at θ ≈ 180° and the strongest positive pressures occurring near θ ≈ 0°.
- AS/NZS 1170.2 does not account for tilt- or density-dependent effects, leading to directionally varying differences in magnitude compared to experimental values.

The results of this study emphasise the need for tilt-, location-, and configuration-specific design guidance to better represent the wind loads acting on rooftop solar arrays installed on low-pitch residential roofs.

These findings suggest the need of improved fixing methodologies, to enable designers to select connection types, batten spacing, and attachment locations that better reflect the wind load demands for high-tilt angles, high-eave, and edge-panel positions.

REFERENCES

ARENA. (2024, 28 March 2024). *$1 billion boost for Australian solar PV manufacturing*. Australian Government Australian Renewable Energy Agency. https://arena.gov.au/news/1-billion-boost-for-australian-solar-pv-manufacturing/#:~:text=%E2%80%9CTo%20date%2C%20ARENA%20has%20invested,a%20domestic%20solar%20manufacturing%20industry.%E2%80%9D

AS/NZS 1170.2. (2021). AS/NZS 1170.2 Wind Actions. In.

Boughton, D. J. F., D.J. Henderson, D.J. Smith, K. Parackal, T. Kloetzke, M. Mason, R. Krupar III, M. Humphreys, S. Navaratnam, G. Bodhinayake, S. Ingham, and J.D. Ginger. (2017). *Tropical Cyclone Debbie Damage to buildings in the Whitsunday Region*.